Pressure induced crystallization in amorphous silicon

K. K. Pandey, [a] Nandini Garg, K. V. Shanavas, Surinder M. Sharma, and S. K. Sikka
High Pressure and Synchrotron Radiation Physics Division, Bhabha Atomic Research Centre, Mumbai 400085, India

(Received 3 March 2011; accepted 18 April 2011; published online 3 June 2011)

We have investigated the high pressure behavior of amorphous silicon (a-Si) using x-ray diffraction and Raman scattering techniques. Our experiments show that a-Si undergoes a polyamorphous transition from the low density amorphous to the high density amorphous phase, followed by pressure induced crystallization to the primitive hexagonal (**ph**) phase. On the release path, the sequence of observed phase transitions depends on whether the pressure is reduced slowly or rapidly. Using the results of our first principles calculations, pressure induced preferential crystallization to the **ph** phase is explained in terms of a thermodynamic model based on phenomenological random nucleation and the growth process. © *2011 American Institute of Physics*. [doi:10.1063/1.3592963]

I. INTRODUCTION

Since the discovery of the high density amorphous (HDA) phase in ice,[1,2] polyamorphic transitions have been extensively studied in ice and other substances, especially those with tetrahedral coordination.[3–6] Silicon, a widely used semiconductor in both its crystalline and its amorphous forms, also undergoes a polyamorphous transition from a tetrahedrally coordinated low density amorphous (LDA) phase to a 5-6 coordinated HDA phase.[7–9] Durandurdu *et al.*[6] have shown theoretically that a very high density amorphous (VHDA) form of silicon (8-9 coordinated VHDA) might also exist.[10] However, experimentally the VHDA phase has not been observed. Instead, HDA has been shown to transform to a crystalline phase under higher pressures. In one of the early reports, Minomura *et al.*[11] showed that amorphous silicon transformed to a mixture of β-Sn and BC8 phases at ~17 GPa. Subsequently, Imai *et al.*[12] carried out white beam x-ray diffraction experiments on amorphous silicon, and, based on only two very weak and broad diffraction peaks, they concluded that it crystallized reversibly to the β-Sn structure at high pressure. However, because the aim of most of these experiments was the observation of a semiconducting to metallic LDA-HDA polyamorphous transition, the crystallization of amorphous silicon (a-Si) was considered a digression. In fact, to the best of our knowledge, to date there is no high resolution diffraction or Raman study on a-Si that could unambiguously help in characterizing the structure of the high pressure phase.

Like polyamorphism, crystallization is also an interesting phenomenon and is one of the most fundamental nonequilibrium phenomena, universal to a variety of materials. The crystalline phase, being a lower energy stable state, can be obtained from the amorphous phase via thermal annealing or mechanical activation. Pressure also influences this thermally induced crystallization process. Most of the experiments imply enhanced thermal stability of the amorphous phase under high pressure, manifested as an increase in the crystallization temperature with pressure.[13–17] However, pressure is also known to reduce the crystallization temperature in some alloys, viz., $Ti_{80}Si_{80}$ (Ref. 18) and Al–La–Ni.[19] Although the suppression or enhancement of crystallization under high pressure has been accounted for in terms of activation energies and diffusivity, the phenomenon is still not fully understood. There are also reports of pressure alone bringing about the crystallization. For example, as is observed in silicon, there are several other materials, such as Zr-based alloys,[20] amorphous Se,[21,22] ice,[23] etc., that crystallize under the influence of pressure alone. An increase in density has been suggested as the driving force for pressure induced crystallization. It is interesting to note that the observation of the polyamorphous phase transition in silicon is similar to that of ice.[23] In view of the fact that Si and ice share some common features (viz., local tetrahedral coordination under ambient conditions, a denser liquid phase, a decreasing melting temperature with pressure), it would be interesting to investigate the crystallization of amorphous Si.

With these motivations, we carried out high pressure angle dispersive x-ray diffraction (ADXRD) and Raman scattering experiments on a-Si up to 45 GPa and 22 GPa, respectively. We have also explained the crystallization of a-Si at high pressure with the help of a thermodynamic model based on the phenomenological random nucleation and growth (RNG) process. First principles calculations were carried out in order to determine the relevant parameters of this model.

II. EXPERIMENTAL DETAILS

The amorphous silicon used in this study was obtained from Bharat Heavy Electricals Limited, India, and was prepared via the plasma enhanced chemical vapor deposition technique. Chemical analysis showed that the sample was 99.9% pure.[24] ADXRD experiments were carried out at the XRD1 beamline of the Elettra synchrotron source using x-rays of wavelength (λ) = 0.6825 Å. Two dimensional x-ray

[a]Electronic mail: kkpandey@barc.gov.in.

diffraction patterns were collected on a MAR345 imaging plate system, calibrated with the help of CeO_2. Amorphous silicon and a small amount of Cu (used as a pressure marker) were loaded into a 100 μm hole drilled in a preindented (40 μm thickness) tungsten gasket of a diamond anvil cell. For these experiments, a 4:1 methanol–ethanol mixture was used as a pressure transmitting medium. The pressure was determined by using the well-known equation of state of copper.[25] These experiments were carried out up to pressures of ~45 GPa. One set of experiments was also carried out up to 23 GPa at the BL10XU beamline of the SPring8 synchrotron ($\lambda = 0.30838$ Å). In this experiment, the pressure was measured using the shifts in the ruby fluorescence lines. Two dimensional images collected on the imaging plates were converted to one dimensional diffraction profiles using FIT2D software.[26] Pair distribution function (pdf) analyses[27,28] of the amorphous phases have been carried out using RAD software.[29] Emerging high pressure crystalline phases were determined by fitting the diffraction data with the help of GSAS software.[30] In addition to ADXRD experiments, high pressure Raman scattering experiments were also carried out on a-Si up to 22 GPa. The Raman spectra were collected in the backscattering geometry using our micro Raman system. The Raman modes were excited using the 532 nm laser light from a solid state laser.

A. Details of *ab initio* calculations

In order to determine some of the parameters used in the thermodynamic analysis of the crystallization of silicon, first principles calculations based on density functional theory, as implemented in the Vienna *Ab Initio* Simulation Package (VASP) (Ref. 31), were also carried out. We employed generalized gradient approximations[32] and the projector augmented wave method[33] to solve Kohn-Sham equations. A Monkhorst-Pack mesh of $8 \times 8 \times 8$ and a kinetic energy cutoff of 380 eV provided good convergence. The energy volume characteristics of the amorphous phase were calculated using a supercell containing 216 atoms and Γ-centered k-point sampling.

The initial structure of the high density amorphous phase was generated by following the methodology outlined in Ref. 34. Because using classical MD in the initial stage could reduce the computational time substantially, we first generated a classical high density amorphous structure at 15 GPa by heating the β-Sn phase up to 3500 K and subsequently quenching the liquid to 500 K at the rate of 1 K/ps. The resultant structure was then equilibrated for several picoseconds using *ab initio* molecular dynamics simulations. Finally, the HDA phase at different pressures was generated by changing the volume and allowing the system to equilibrate for 0.5 ps. The Birch-Murnaghan equation of state[35] was fitted to get pressure–volume values at lower pressures.

III. RESULTS AND DISCUSSION

A. Results

In agreement with past studies,[8,9] our high pressure x-ray diffraction experiments on bulk amorphous Si also show

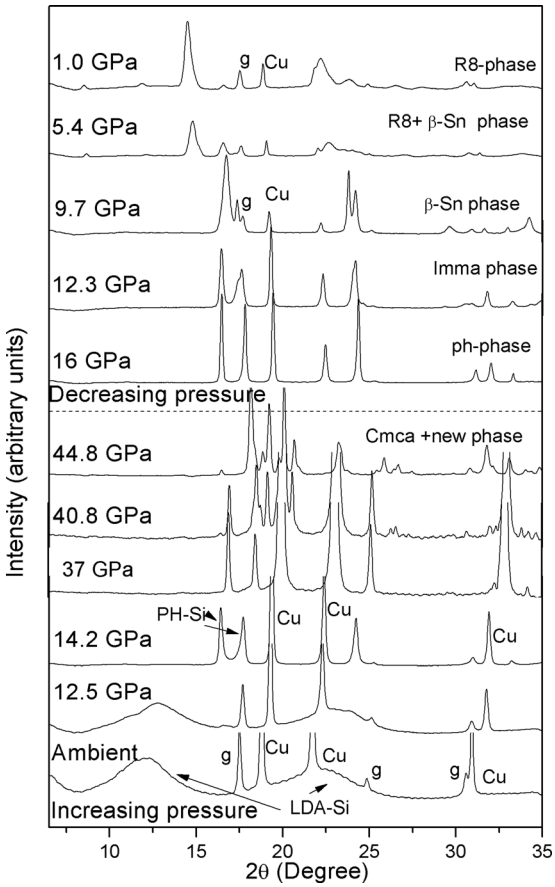

FIG. 1. X-ray diffraction patterns of amorphous silicon at different pressures in the first experimental run. The diffraction patterns shown above the dotted line correspond to released pressure runs. In this run, the pressure was released in small pressure steps.

a LDA-HDA transformation (Figs. 1–5). This transformation is evident from pdf analyses of our ADXRD data. At high pressure, the Q range was limited (60 nm^{-1}), and thus the long wavelength components were dominant. Because of this, we missed the finer details of the pair distribution function. However, we were able to see the variation in the nearest neighbor distance (NND), which at ambient pressure is ~2.32 Å. This represents the Si–Si bond length in tetrahedral coordination. The NND at different representative pressures is given in Table I. As expected, the Si–Si NND first decreases with pressure and then increases slightly above 12 GPa. The increase in the Si–Si bond distance indicates that the Si–Si coordination must have increased. Therefore, from our pdf studies we can say that LDA silicon transforms to HDA above ~12 GPa. Our Raman studies are in agreement with the pdf analysis (Figs. 4 and 5). The broad band centered at ~480 cm^{-1} in the LDA phase broadens beyond 12 GPa and extends from 200 cm^{-1} to 700 cm^{-1} in the HDA phase. This observation is similar to that of McMillan *et al.*[8]

Upon a further increase of the pressure, HDA-Si crystallizes at ~14 GPa, as can be seen from the x-ray diffraction data of Figs. 1 and 3. However, unlike in previous studies[11,12] in which the high pressure crystalline phase was reported to be β-Sn, we found that the structure of this crystalline phase was similar to that of the primitive hexagonal (**ph**) phase.[36] Figure 2 shows the Rietveld refinement of

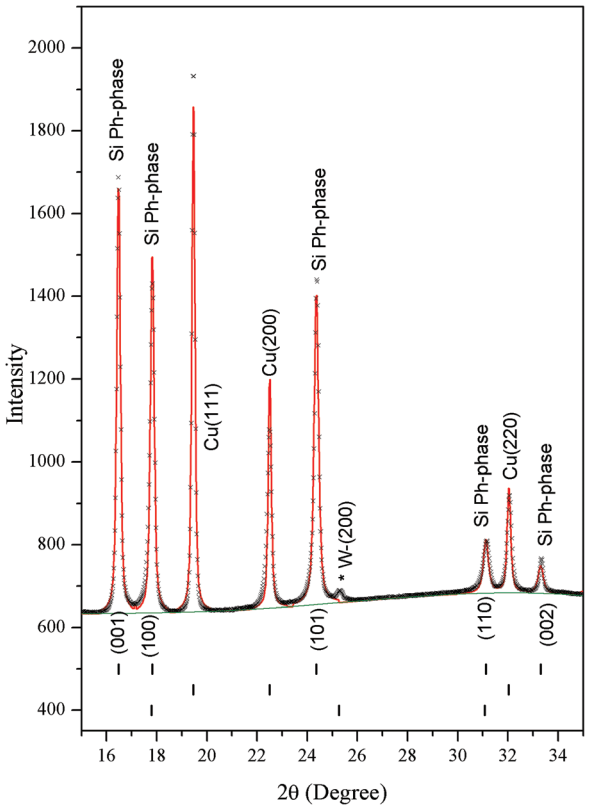

FIG. 2. (Color online) Rietveld refinement of the diffraction pattern at 16.8 GPa showing the high pressure crystalline phase to be primitive hexagonal (**ph**). Additional peaks correspond to Cu, the pressure calibrant, and W, the gasket material.

diffraction data at 16.8 GPa, indicating that the high pressure phase is the **ph** phase. This misinterpretation of the structure of the high pressure crystalline phase in past studies could be due to poorly resolved diffraction data. Also, the close resemblance between the diffraction patterns of the **ph** and β-Sn phases over the limited 2θ range, generally available in

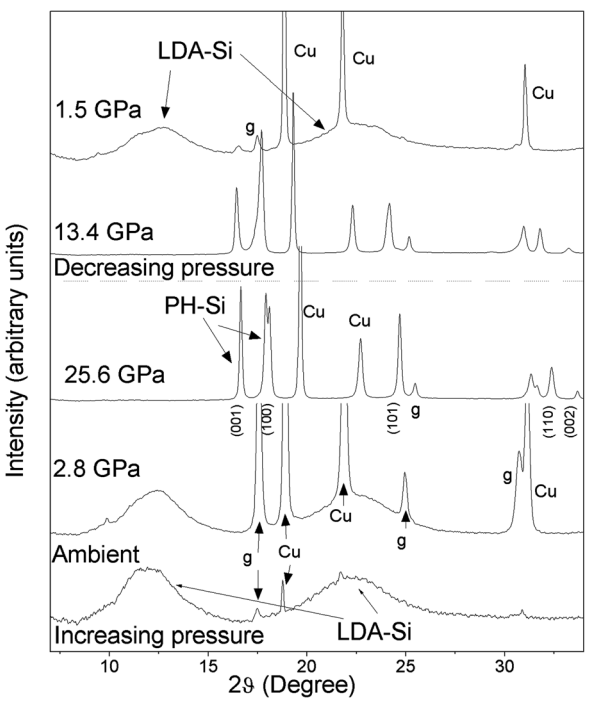

FIG. 3. X-ray diffraction patterns of bulk amorphous silicon at different pressures in the second experimental run. The diffraction patterns shown above the dotted line correspond to released pressure runs. In this run, the pressure release was abrupt.

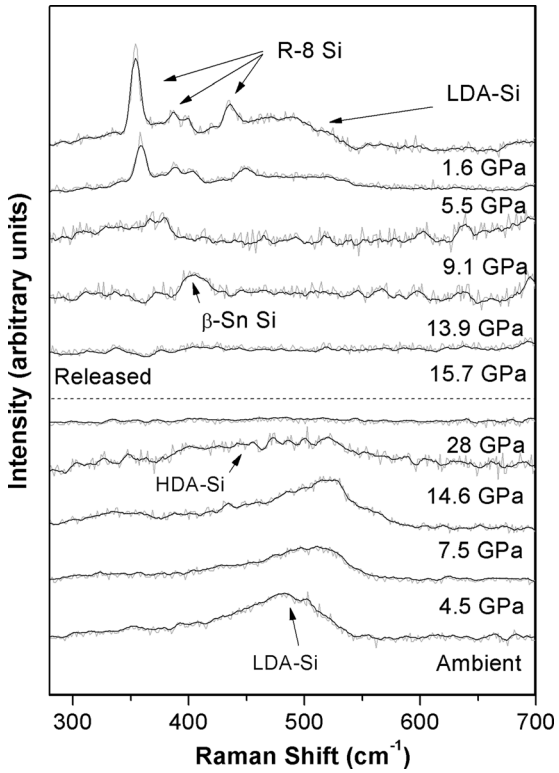

FIG. 4. Raman spectra of a-Si at a few representative pressures when the pressure was released in small steps. The Raman spectra shown above the dotted line correspond to released pressure runs.

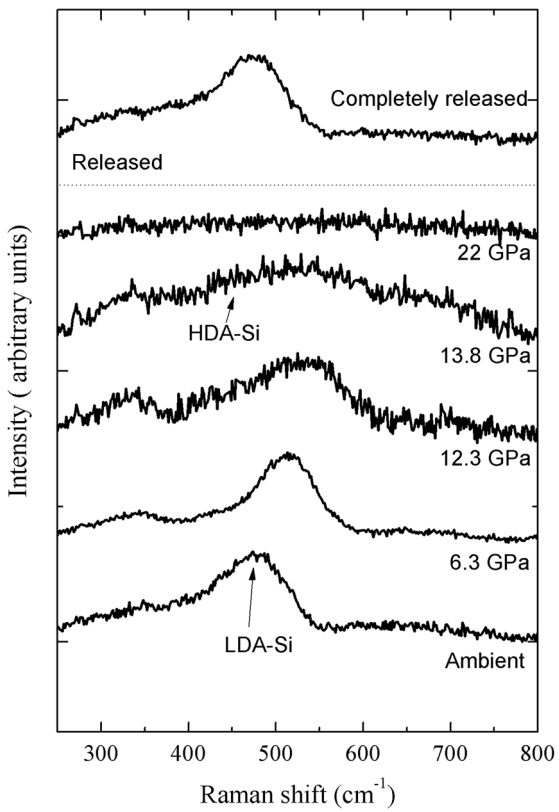

FIG. 5. Raman spectra of a-Si at a few pressures when the pressure was released abruptly.

TABLE I. Nearest neighbor distance from pair distribution analysis at different representative pressures.

Pressure (GPa)	Nearest neighbor distance (Å)
Ambient	2.32
12.6	2.15
13.6	2.22

high pressure experiments, would have further aggravated the situation. With well resolved diffraction data, obtained through high brilliance synchrotron sources such as SPring8 and Elettra, and a powerful structural refinement technique (viz., Rietveld refinement), we have been able to correctly identify the crystalline phase as **ph**. Because the **ph** phase does not have any active Raman mode, our Raman measurements also agree with this observation, as we do not see any vibration mode above the crystallization pressure. Moreover, if the high pressure crystalline phase were the β-Sn phase, we would have observed a Raman band close to $\sim$350 cm^{-1}.

On further pressurizing of the **ph** phase, we observed (Fig. 1) that it undergoes a phase transformation to a mixture of Cmca and a new phase at $\sim$40 GPa. Rietveld analysis shows that this phase is different from the hexagonal close pack (HCP) (Ref. 24) or Cmca phase observed previously for bulk crystalline Si. However, due to poor statistics and overlapping peaks, the structure of this new phase could not be identified. It might be a lower symmetry structure derived from the Cmca or HCP phase, and it could have been stabilized because of remnant defects in the preceding high pressure crystalline phases obtained from bulk amorphous silicon.

Released pressure runs are more dramatic in the sense that, depending upon the rate of the release of pressure, the **ph** phase transforms back to the initial amorphous phase or undergoes several phase transformations as observed in bulk crystalline silicon (Figs. 1 and 3). It can be seen in Fig. 1 that if the pressure is released slowly, then the **ph** phase transforms to the Imma phase at $\sim$12.3 GPa, to the β-Sn structure at $\sim$10 GPa, and finally to the R-8 phase at $\sim$5.5 GPa. Signatures of R-8 are also evident in the Raman spectra of a-Si in the slow release run (Fig. 4). The BC-8 phase, which is observed on the release of pressure in bulk crystalline Si,[37] was not observed in our study upon the complete release of pressure. On the fast release of pressure from the **ph** phase obtained in a-Si, it transforms to an initial LDA phase, as can be clearly seen in both x-ray diffraction and Raman measurements (Figs. 3 and 5). It is interesting to note that a similar recovery of LDA-Si has also been observed in Si nano-particles[38] and porous Si.[5,39] However, there the results were independent of the rate of the release of pressure. Amorphous-Si, being a metastable phase in the bulk system under ambient conditions, can be obtained only by kinetically trapping it upon the release of high pressure, and that too is only under certain circumstances.[40]

On re-pressurizing the R-8 phase, we observed (Fig. 6) that it transformed to beta tin at $\sim$13 GPa, which further transformed to the **ph** phase at $\sim$19 GPa. These results indicate that on the release of pressure, the **ph** phase, crystallized from amorphous silicon, exhibits a behavior similar to that of bulk crystalline silicon.[24,41–43]

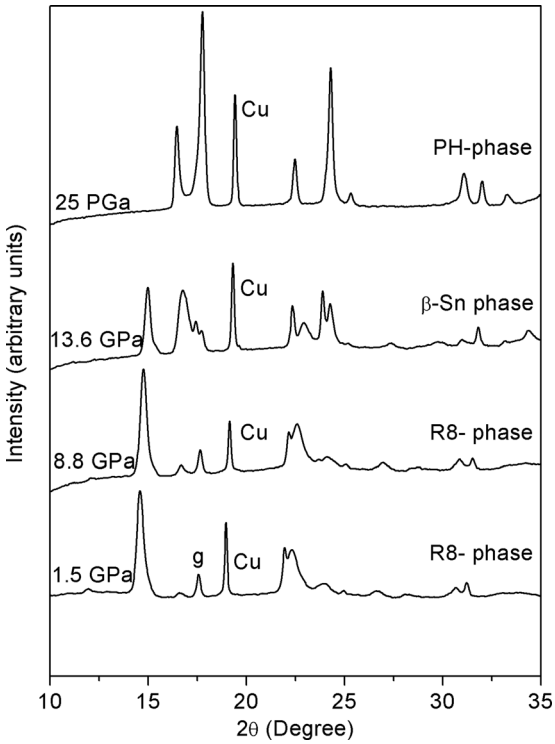

FIG. 6. X-ray diffraction patterns of recycled pressure runs of the R8 phase of silicon obtained from the slow pressure release of amorphous Si.

B. Thermodynamic analysis

Our experimental observations suggest that the crystallization path from the amorphous (HDA-Si) to the **ph** phase might have a low activation barrier as compared to the paths leading to other crystalline phases or to the VHDA phase. This phase, being energetically as well as kinetically preferred, is also supported by our observation that, irrespective of the rate of the pressure increase, a-Si always crystallizes into the **ph** phase. To explain this preferential crystallization to the **ph** phase, we present here a thermodynamic model based on the phenomenological random nucleation and growth process.[44–46] A reassuring aspect of this analysis is that all of the relevant parameters used in our random nucleation and growth modelings were derived from the density functional theory based first principles calculations.

The crystallization of an amorphous phase is usually a first order reconstructive phase transition involving discontinuous volume change and rigorous atomic rearrangements. These rearrangements require some energy to overcome the energy barrier that the system faces in the path of transformation from the amorphous to the crystalline phase. At high temperatures, this is provided by the thermal energy, which also facilitates the diffusion of atoms. The mechanism of transformation is generally nucleation and growth instead of transformation of the system as a whole, as the nucleation of small clusters requires less energy. Nucleation can be heterogeneous (nucleation at impurity or defect sites) or homogeneous (appearing entirely due to thermal fluctuations).

At high pressures, the diffusion of atoms is hindered because of steric constraints. Also, the steepening of interatomic potentials reduces thermal fluctuations. This should,

in principle, deter crystallization of the amorphous phase at high pressures. However, in disagreement with this hypothesis, as mentioned above, there are several experimental reports on the pressure induced crystallization of amorphous materials. In the absence of long range diffusion, this pressure induced crystallization should be achievable only in those systems where crystallization takes place through local atomic rearrangements. Hence, only polymorphous crystallization, in which there is no compositional difference between the parent and daughter phases, may be feasible under high pressure. Because Si also belongs to the category of polymorphous crystallization, the nucleation and growth model can be used to explain pressure induced crystallization in Si. For simplicity, we have considered homogeneous nucleation.

In the random nucleation and growth process, finite crystalline nuclei are formed in the amorphous matrix as a result of thermal fluctuations. The Gibbs free energy change for the formation of a spherical crystalline nucleus in an amorphous matrix is given as

$$\Delta G^n(T,P) = \frac{(1/6)\pi d^3}{V^c}(\Delta G^{am\to c} + E) + \pi d^2\sigma, \qquad (1)$$

where $\Delta G^{am\to c}$ is the molar free energy change for the transformation from the amorphous to the crystalline phase, σ is the free energy increase for forming the unit area on the crystal-amorphous interface, V^c is the molar volume of the crystalline phase, and E is the elastic energy induced by the volume change during the phase transition. E can be neglected, as its effect on the free energy change during the nucleation process is generally very small.[47] Because the crystalline phase has a lower energy than the amorphous phase, the volume part (i.e., the first term) decreases ΔG^n, whereas the surface part (i.e., the second term), which is due to the formation of an interface between the crystalline nuclei and the surrounding amorphous matrix, always increases ΔG^n. Therefore, for a certain critical diameter (d_c) of the nuclei, ΔG^n is at a maximum, which is also known as nucleation work ΔG^*. This is given as

$$\Delta G^* = \frac{16\pi\sigma^3}{3(\Delta G^{am\to c}/V^c)^2}. \qquad (2)$$

The corresponding d_c is given as

$$d_c = \frac{\sigma}{(\Delta G^{am\to c}/V^c)}. \qquad (3)$$

Only nuclei having a diameter above d_c grow subsequently, and eventually the crystallization occurs. The steady state rate of such nuclei formation is given as[48]

$$I_{st} = I_o \exp\left[-\frac{\Delta G^* + \Delta G_D}{k_B T}\right]. \qquad (4)$$

It determines the number of supercritical clusters formed per unit time in the unit volume of the system. Here ΔG_D is the activation free energy for the transfer of a "structural unit" from the amorphous to a crystalline phase. The pre-exponential term I_o in Eq. (4) depends weakly only on temperature and varies between 10^{41} and 10^{43} m^{-3} s^{-1} for various condensed systems.[49] It is given as

$$I_o = 2N\frac{k_B T}{h}\left(\frac{a^2\sigma}{k_B T}\right)^{1/2}, \qquad (5)$$

where $N \sim 1/a^3$ is the number of structural (formula) units with a mean size a.

To understand the crystallization of silicon at high pressure, we need to know the nucleation work ΔG^*, the critical diameter d_c, and the steady state nucleation rate as a function of pressure. At pressures above 10 GPa, there are three competing phases, viz., the β-Sn, Imma, and **ph** phases. Because Imma is very close to the β-Sn phase both energetically and structurally,[50] we have compared the crystallization process from the HDA phase of amorphous Si to the β-Sn and **ph** phases only. In order to determine some of the parameters (viz., the molar volumes of different amorphous and crystalline phases used in calculating these quantities), we carried out *ab initio* calculations on different phases of silicon. The interfacial energy per unit area σ was taken to be 0.49 J/m^2, which is quite close to the solid liquid interface energy of silicon.[51] The enthalpy at T = 0 K was used to estimate the nucleation work.[52] The calculated equations of states, shown in Fig. 7 for different phases of silicon, were used to find the molar volumes V^c and V^{am} as a function of the pressure. The consequent variation of the critical diameter d_c is shown in Fig. 8. We note that d_c decreases with pressure for both the crystallizable phases (i.e., β-Sn) and the primitive hexagonal phase. At ambient pressure, d_c was higher for the **ph** phase; however, at higher pressures, the d_c for the **ph** phase becomes smaller than that for the β-Sn phase. In Fig. 9 we show the nucleation work ΔG^* required for crystallization from the amorphous to the β-Sn, as well as to the **ph**, phase. We can see that ΔG^* for crystallization to the **ph** phase is initially higher than that required to crystallize the β-Sn phase. However, similar to the behavior of d_c, beyond 5 GPa it becomes lower, and at 14 GPa (the experimentally observed transition pressure in the present study) it is ~20% lower than the nucleation work required for the crystallization of the β-Sn phase. This difference in the nucleation work results in a much higher nucleation rate in the case of crystallization

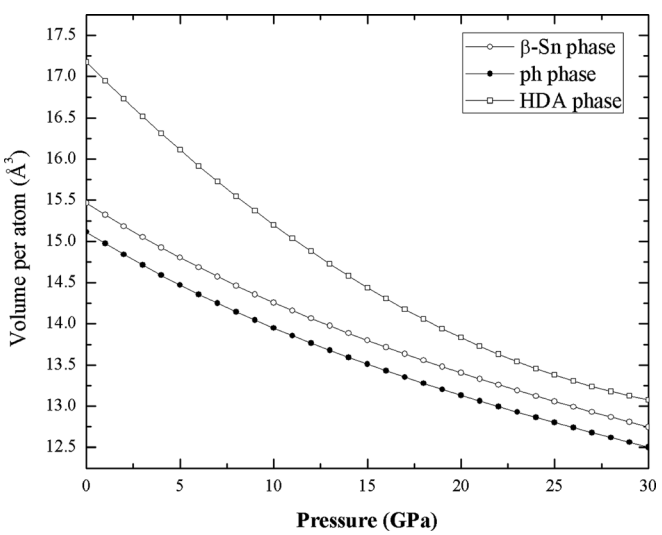

FIG. 7. Equation of state obtained from first principles calculations for different crystalline and amorphous phases of Si.

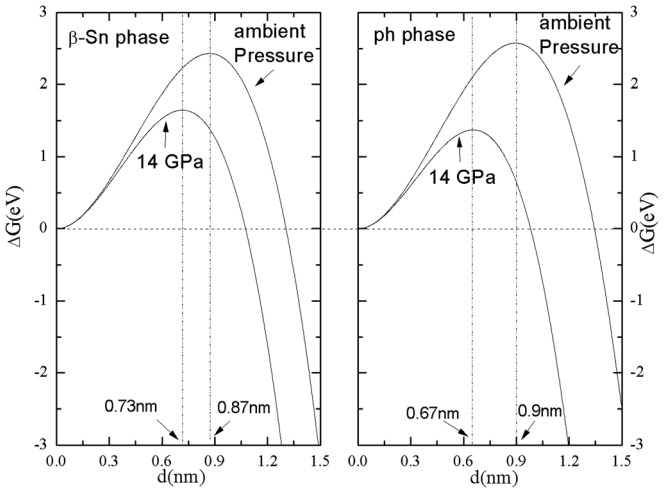

FIG. 8. Gibbs free energy change ΔG as a function of nucleus diameter at ambient pressure and 14 GPa.

to the ph phase than in the case of crystallization to the β-Sn phase. In order to compare the nucleation rates in these two cases, we have assumed the same exponential prefactor I_o and activation barrier ΔG_D for both cases. As shown in Fig. 10, at around 14 GPa the steady state nucleation rate is very large (about four orders of magnitude higher) in the case of crystallization to the **ph** phase, establishing the preferred growth of this phase.

Though this model reasonably explains the preferred crystallization to the **ph** phase, the very basic assumption of the RNG process (i.e., the infinitesimal thickness of the interface between crystalline nuclei and the amorphous matrix) needs to be reviewed. This approximation is valid in the case of crystallization from the super cooled molten state, as in that case the relaxation times are very small. In the case of crystallization from amorphous solids, where relaxation times may be relatively larger, finite thickness of the interface might not be avoidable. This will introduce an additional $P\Delta V$ term in Eq. (1), in which ΔV corresponds to the volume change due to the crystal interface formation.[21] This

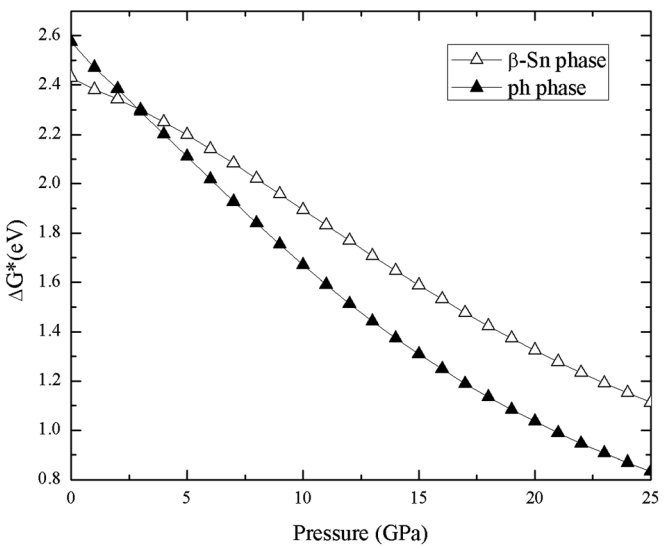

FIG. 9. Nucleation work (ΔG^*) for crystallization from amorphous Si to different crystalline phases of Si.

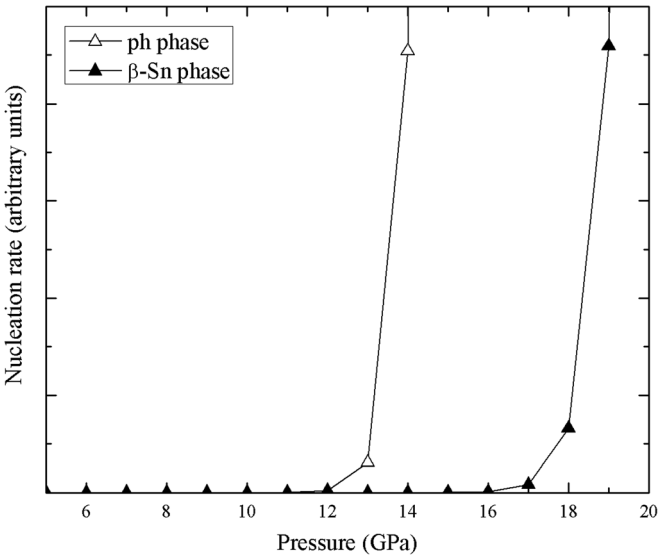

FIG. 10. Relative steady state nucleation rate (I/I_0) for crystallization from amorphous Si to different crystalline phases of Si.

volume change depends on the size of the nucleus, the thickness of interface, and the molar volumes of the amorphous and interface regions. For positive values of $\Delta V(d_c)$, the applied pressure will enhance the free-energy change ΔG^n and thus will retard crystallization, whereas negative values will support the crystallization process. The role of the crystal-amorphous interface and, thus, the $P\Delta V$ term have been very effectively used to explain the initial increase and subsequent reduction of the crystallization temperature for amorphous Se under high pressure by Ye and Lu.[21] However, they have assumed a constant interface thickness under pressure and have approximated the molar volume of the interface region from the ratio of excess enthalpies of the interface and the amorphous region. In view of the fact that the crystallization pressure for amorphous Se is very close to the pressure at which the molar volume of the amorphous phase becomes lower than that of the crystalline phase, it seems that the relative molar volumes of the crystalline and amorphous phases play a significant role in the crystallization process. The role of the interface molar volume seems to be more prominent at lower pressures, where the crystal-amorphous interface has a lower coordination than both the crystalline and the amorphous phases, and it therefore results in volume expansion. At high pressures, where the amorphous and crystalline phases have very close densities, the interface molar volume should be somewhere in between those of the crystalline and amorphous phases. In fact, our recent classical molecular dynamic simulations of the solid phase epitaxial growth of the β-Sn phase on HDA-Si show an intermediate Voronoi volume for the Si atoms in the interface region.[34] This suggests that the $P\Delta V$ term for crystallization from the HDA-phase in Si will always be negative and enhance the crystallization process in amorphous Si under high pressure. Hence, the qualitative behavior would still be similar even if we considered a finite thickness of the interface region. However, for a detailed quantitative analysis, one needs to know the correct behavior of the interface thickness and its molar volume as a function of the pressure.

Extensive molecular dynamics simulations would further improve our microscopic understanding of the crystallization process in amorphous Si.

IV. CONCLUSION

Our studies on amorphous silicon have shown that it undergoes a LDA to HDA transition, followed by pressure induced crystallization to the **ph** phase. Upon an increase of the pressure, this **ph** phase transforms to a mixture of Cmca and a new phase phase at ~40 GPa. The preferred crystallization of a-Si to the **ph** phase in the pressure region in which other crystalline phases of Si (viz., β-Sn and Imma) are also stable has been explained by invoking the thermodynamical model based on the random nucleation and growth process. The parameters for the thermodynamic analysis were derived from first principles calculations.

ACKNOWLEDGMENTS

The authors are thankful to Dr. Maurizio Polenturutti and Giorgio for their help while we were carrying out these experiments at the XRD1 beamline at Elettra Synchrotron. The authors would also like to thank Dr. Ohishi and Dr. Hirao for their help while we carried out these experiments at BL10XU SPring8.

[1]O. Mishima, L. D. Calvert, and E. Whalley, Nature **310**, 393 (1984).
[2]O. Mishima, L. D. Calvert, and E. Whalley, Nature **314**, 314 (1985).
[3]O. Mishima and H. E. Stanley, Nature **396**, 329 (1998).
[4]D. J. Lacks, Phys. Rev. Lett. **84**, 4629 (2000).
[5]S. K. Deb, M. C. Wilding, M. Somayazulu, and P. F. McMillan, Nature **414**, 528 (2001).
[6]M. Durandurdu and D. A Drabold, Phys. Rev. B **64**, 014101 (2001).
[7]M. Durandurdu and D. A. Drabold, Phys. Rev. B **66**, 205204 (2003).
[8]P. F. McMillan, M. Wilson, D. Daisenberger, and D. Machon, Nature Mater. **4**, 680 (2005).
[9]D. Daisenberger, M. Wilson, P. F. McMillan, R. Queseda Cabrera, M. C. Wilding, and D. Machon, Phys. Rev. B **75**, 224118 (2007).
[10]T. Morishita, Phys. Rev. Lett. **93**, 055503 (2004).
[11]S. Minomura, Semicond. Semimetals **21A**, 273 (1984).
[12]M. Imai, T. Mitamura, K. Yaoita, and K. Tsuji, High Press. Res. **15**, 167 (1996).
[13]W. C. Emmens, J. Vrigen, and S. Radelaar, J. Non-Cryst. Solids **18**, 299 (1975).
[14]H. Iwasaki and T. Masumoto, J. Mater. Sci. **13**, 2171 (1978).
[15]T. Imura, M. Suwa, and K. Fujii, Mater. Sci. Eng. **97**, 247 (1988).
[16]W. K. Wang, H. Iwasaki, and K. Fukamichi, J. Mater. Sci. **15**, 2701 (1980).
[17]F. Ye and K. Lu, Acta Mater. **46**, 5965 (1998).
[18]W. K. Wang, H. Iwasaki, C. Suryanarayana, and T. Masumoto, J. Mater. Sci. **18**, 3765 (1983).
[19]F. Ye and K. Lu, Acta Mater. **47**, 2449 (1999).
[20]D. He, Q. Zhao, W. H. Wang, R. Z. Che, J. Liu, X. J. Luo, and W. K. Wang, J. Non-Cryst. Solids **297**, 84 (2002).
[21]F. Ye and K. Lu, Phys. Rev. B **60**, 7018 (1999).
[22]H. Liu, L. Wang, X. Xiao, F. De Carlo, J. Feng, H.-K. Mao, and R. J. Hemley, Proc. Natl. Acad. Sci. U.S.A. **105**, 13229 (2008).
[23]R. J. Hemley, L. C. Chen, and H. K. Mao, Nature **338**, 638 (1989).
[24]Ambient condition FTIR and Raman spectra indicated that it had some hydrogen and oxygen impurities.
[25]H. K. Mao, J. Xu, and P. M. Bell, J. Geophys. Res. **91**, 4673 (1986).
[26]A. P. Hammersley, S. O. Svensson, M. Hanfland, A. N. Fitch, and D. Hausserman, High Press. Res. **14**, 235 (1996).
[27]V. Petkov, P. N. Trikalitis, E. S. Bozin, S. J. L. Billinge, T. Vogt, and M. G. Kanatzidis, J. Am. Chem. Soc. **124**, 10157 (2002).
[28]S. J. L. Billinge and M. G. Kanatzidis, Chem. Commun. (Cambridge) 749 (2004).
[29]V. Petkov, J. Appl. Cryst. **22**, 387 (1989).
[30]A. C. Larson and R. B. Von Dreele, "General Structure Analysis System (gsas)," Los Alamos National Laboratory Report LAUR 86–748, (2004).
[31]G. Kresse and J. Hafner, Phys. Rev. B **47**, R558 (1993); G. Kresse and J. Furthmüller, *ibid*. **54**, 11169 (1996).
[32]J. P. Perdew, K. Burke, and Y. Wang, Phys. Rev. B **54**, 16533 (1996); J. P. Perdew, K. Burke, and M. Ernzerhof, Phys. Rev. Lett. **77**, 3865 (1996).
[33]P. E. Blöchl, Phys. Rev. B **50**, 17953 (1994).
[34]K. V. Shanavas, K. K. Pandey, N. Garg, and S. M. Sharma, "Computer simulations of crystallization kinetics in amorphous silicon under pressure".
[35]F. Birch, Phys. Rev. **71**, 809 (1947).
[36]H. Olijnyk, S. K. Sikka, and W. B. Holzapfel, Phys. Lett. **103A**, 137 (1984).
[37]R. H. Wentorf and J. S. Kasper, Science **139**, 338 (1963); F. P. Bundy, J. Chem. Phys. **41**, 3809 (1964).
[38]S. H. Tolbert, A. B. Herhold, L. E. Brus, and A. P. Alivisatos, Phys. Rev. Lett. **76**, 4384 (1996).
[39]N. Garg, K. K. Pandey, K. V. Shanavas, C. A. Betty, and S. M. Sharma, Phys. Rev. B. **83**, 115202 (2011).
[40]M. Imai, K. Yaoita, Y. Katayama, J. Q. Chen, and K. Tsuji, J. Non-Cryst. Solids **150**, 49 (1992).
[41]J. C. Jamieson, Science **139**, 762 (1963).
[42]J. Z. Hu and I. L. Spain, Solid State Commun. **51**, 263 (1984).
[43]M. I. McMahon and R. J. Nelmes, Phys. Rev. B. **47**, 8337 (1993).
[44]P. G. Debenedetti, *Metastable Liquids: Concepts and Principles* (Princeton University Press, Princeton, NJ, 1996), pp. 146–199.
[45]A. Onuki, *Phase Transition Dynamics* (Cambridge University Press, Cambridge, England, 2002), pp. 488–551.
[46]D. Turnbull, Contemp. Phys. **10**, 473 (1969).
[47]F. Ye and K. Lu, Acta Mater. **46**, 5965 (1998).
[48]I. Gutzaw and J. Schmelzer, *The Vitreous State: Thermodynamics, Structure, Rheology and Crystallization* (Springer, Berlin, 1995).
[49]J. W. Christian, *Transformations in Metals and Alloys, Part I* (Pergamon, Oxford, England, 1981).
[50]S. M. Sharma and S. K. Sikka, J. Phys. Chem. Solids **46**, 477 (1985).
[51]N. Bernstein and M. J. Aziz, Phys. Rev. B **58**, 4579 (1998).
[52]We have approximated the Gibbs free energy to the enthalpy at $T=0$ K for estimating the nucleation work, assuming the similar qualitative behavior of both of these energies under pressure.